PHYSICAL REVIEW B VOLUME 23, NUMBER 11 1 JUNE 1981

Compound geometrical resonances in superconducting Zn-Pb film sandwiches

L. Wong,* S. Shih, and W. J. Tomasch
Department of Physics, University of Notre Dame, Notre Dame, Indiana 46556
(Received 29 September 1980)

Thick, clean Zn films, when backed by clean Pb films of sufficient thickness, produce first-derivative tunneling spectra that differ markedly from the predictions of Wolfram's theory in the central virtual-state region. Gallagher has recently extended Wolfram's theory to allow for quasiparticle geometrical resonances in both metal layers, and, using his results, we are able to explain the anomalous portions of our spectra, as well as those portions which continue to agree with Wolfram's theory. For the c-axis orientation of Zn and the [111] orientation of Pb, we obtain Fermi velocities of $(1.31 \pm 0.020) \times 10^6$ and $(0.78 \pm 0.04) \times 10^6$ m/s, respectively. Our estimate of the Zn electron-phonon coupling parameter, $\lambda = Z_N(0) - 1 = 0.42$, agrees with theoretical estimates by Tomlinson and Swihart, but away from the Fermi surface our estimates of the complex renormalization function generally exceed theirs.

I. INTRODUCTION

Real metals have their electronic properties determined in part by the electron-phonon interaction, which alters quasiparticle lifetimes and energies, and thereby induces mass renormalizations. Electronic tunneling experiments performed with superconductors can probe this interaction quite directly, yielding estimates of the renormalization function, $Z(E)$, whose real part yields energy-dependent mass enhancements, and whose imaginary part determines the coupled phonon spectrum $\alpha^2F(\omega)$. Renormalized group velocities inferred from our geometrical resonance measurements do not represent averages over Landau orbits on the Fermi surface, but instead represent averages over small patches of constant energy surfaces and extend to about 6 meV above the Fermi surface.

When micrometer-thick films of clean Zn (metal N) are backed by Pb (metal S) and maintained at low temperature, first-derivative tunneling spectra acquired at the N-metal surface[1–3] contain structure related to bound-state levels (BSL) and virtual-state levels (VSL) caused by Andreev scattering[4] at the N-S interface. The general tendency for virtual-state derivative spectra (VSDS) to exhibit level spacings that scale inversely with N-layer thickness, d_N, suggests a quasiparticle standing-wave picture in which VSL structure corresponds to geometrical scattering resonances. Wolfram's theory,[5] which describes N-layer resonances induced by contact with metal S, provides good single-band fits for many of our Zn-Pb sandwiches[3] and, for these, yields a consistent Zn Fermi velocity. For the remainder, Wolfram's theory continues to describe the BSL and upper VSL spectrum, but fails to explain new complexities in the central VSL spectrum.

Gallagher[6] has recently extended Wolfram's model to allow for geometrical resonances in both metal layers; and when metal S is sufficiently thick and clean, his theory predicts compound resonances that (1) characterize the N-S sandwiches as a whole and that (2) differ substantially from Wolfram's spectrum. Using Gallagher's theory, we are able to explain our VSL anomalies and to regain the Zn Fermi velocity inferred in their absence. In the process, we also extract estimates of the Pb Fermi velocity and of the complex renormalization function, $Z_N(E)$, for Zn. Although our value of $Z_N(0)$ compares favorably with that calculated by Tomlinson and Swihart,[7] our estimates away from the Fermi surface ($E \gtrsim 3$ meV) generally exceed theirs.

II. EXPERIMENTAL METHOD

Metal films for our Al-ZnO-Zn-Pb diodes are evaporated onto glass substrates situated inside a modular vacuum system constructed from six-inch-diameter glass pipe fittings joined together by elastomer seals. Besides the usual baffles ($T \simeq 283$ K) and traps (77 K) associated with large oil diffusion pumps (2000 l/s), this system incorporates additional baffles (283 K), to isolate evaporation sources from one another, and a cylindrical Meissner trap (77 K) to define the working volume. We routinely cool the substrate holder with liquid nitrogen about 10 min before a Pb evaporation, since chilled substrates promote film sticking and smoothness. Newly deposited Pb films are promptly exposed to a preestablished Zn flux, thereby minimizing the opportunity for contaminating the Zn-Pb interface. Both evaporations proceed at similar rates (200–400 Å/s), and pressures during a typical Zn evaporation may rise from

0.2 to 1.5 μTorr. Since both metals must have long mean free paths (MFP) and must make clean contact if compound resonances are to occur at all, the observation of strong compound resonances justifies our technique. (We will infer MFP's of 4–7 μm for Zn and 1–5 μm for Pb.) After resting in vacuum ($P \simeq 0.07$ μTorr) for roughly an hour, completed sandwiches are exposed briefly ($\simeq 5$ min) to ultrahigh-purity oxygen, removed to permit painting of all prospective junction edges with Formvar, and replaced to permit evaporation of Al counterelectrodes (CE). (We choose Al because of its good resolution and lack of troublesome phonon structure.) Three of the six newly completed tunnel diodes are then promptly transferred to our ^{3}He refrigerator, where cooling to 77 K starts within 20 min of diode completion. X-ray-diffractometer measurements, carried out on several diodes used in tunneling experiments, confirm that Zn and Pb, respectively, have the strong c axis and [111] fiber textures anticipated. All film thicknesses are measured by optical interferometry.

Although most sandwiches that produce strong VSDS structure also produce strong compound resonance effects, we have occasionally encountered spectra that obey Wolfram's theory at all biases. Since the Pb films in these instances are still reasonably thick ($d_S \leq 0.3$ μm), this behavior suggests that they are also reasonably rough or have insufficient MFP's. Sandwiches lacking compound resonances have one (atypical) factor in common: substrate cooling was reinitiated early during the Zn evaporation. Despite a lack of direct evidence, we suspect that our thinner Pb films ($d_S \leq 0.3$ μm), owing to their deposition onto chilled substrates, generally begin in a finely polycrystalline state and that heat from the subsequent Zn evaporation promotes grain growth and MFP improvement—unless prevented by additional substrate cooling.

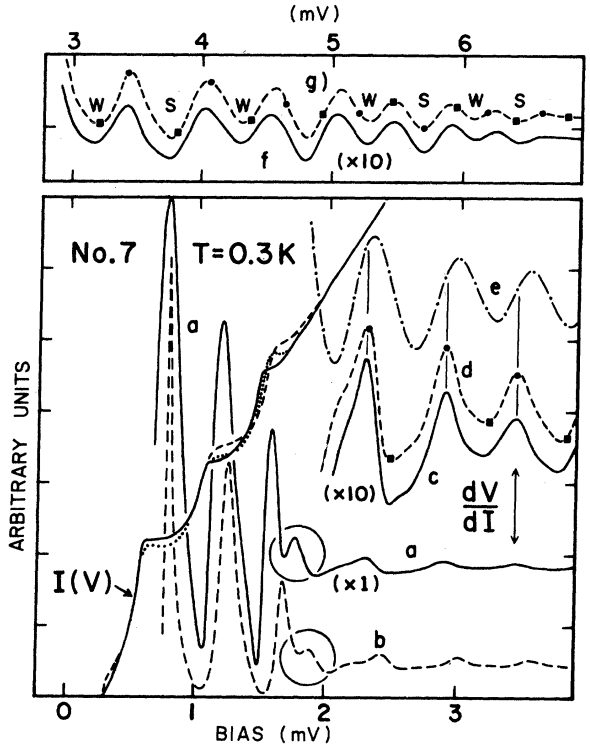

FIG. 1. Tunneling measurements (solid curves) acquired with 2.16 μm of Zn backed by 1.22 μm of Pb. Compound resonances in the dV/dI spectrum occur for biases eV $\simeq$ 1.6–4.0 meV. Theoretical spectra (broken curves) predicted by Gallagher's theory (b, d, and g) and by Wolfram's theory (e and g above $\simeq$4.0 meV) are all computed for $C_N Z_N(0) = 1.56$ meV^{-1}. Gallagher's prediction b accounts for the first (encircled) virtual state a, and Wolfram's e does not. Theoretical currents, which below $\simeq$1.6 meV are the same for both theories, correspond to $C_N Z_N(0)$ values of 1.71 (dotted curve) and 1.56 (dashed curve). Strong (S) and weak (W) minima are labeled for curve g, as are bias locations of maxima (●) and minima (■) anticipated from Tomlinson and Swihart's renormalization (Refs. 7 and 16).

III. EXPERIMENT VERSUS WOLFRAM THEORY

Experimental $I(V)$ and VSDS results, obtained with 2.16 μm of Zn backed by 1.22 μm of Pb, appear as solid curves in Fig. 1. Leakage currents, by their smallness, indicate charge transfer that proceeds almost entirely by tunneling. The eight junctions that produce VSL spectra with compound resonances also produce BSL structure strong enough to be discerned as steps in $I(V)$. When interference effects reach these proportions, formation of the first BSL peak in the N-metal density of states, $N(E)$,[8] causes substantial reductions in $N(E)$ at and near the gap edge ($E = \Delta_N$). Consequently, the usual abrupt rise in current (near eV $= \Delta_{CE} + \Delta_N \simeq 0.4$ meV) associated with the gap edge gives way to a more gradual rise at a higher bias ($\simeq 0.8$ meV) associated with the first BSL peak.[9] Similarly, subsequent BSL peaks and intervening minima produce current step risers and intervening step treads, and these add dips and peaks to dV/dI (curve a). The computed $I(V)$ curves of Fig. 1 (dashes and dots), which result from the use of either theory, illustrate the latitude available in fitting observed currents. Above eV $\simeq$ 1.6 meV ($\simeq \Delta_{CE} + \Delta_S$), quasiparticles are no longer confined to Zn by total internal reflection, which occurs at lower biases because of the absence of states in the Pb gap, and an abrupt drop in derivative amplitudes

(curve a) marks entry into the VSL regime. Finally, above eV $\simeq$ 6.5 meV spontaneous phonon emission in Zn quenches all quasiparticle interference effects.

Intercomparison of experimental VSDS line shapes, as a function of bias (Fig. 1, curves c and f), discloses that those above eV $\simeq$ 4.0 meV are simpler than those at lower biases, say 2.0–4.0 meV. Above $\simeq$4.0 meV, where spontaneous phonon emission in Pb prevents geometrical resonances in the Pb layer[10,11] and VSDS results computed from Gallagher's theory (curve g) reduce to Wolfram's, comparison with experiment (curve f) demonstrates the continued success of Wolfram's theory. At lower biases, however, a corresponding comparison (curve e vs c) shows that line shapes and peak locations are no longer predicted correctly. Inability to account for the lowest-lying VSDS peak—the encircled feature of curve—emphasizes the extent of these difficulties. A second set of tunneling characteristics, these acquired with 1.35 μm of Zn backed by 1.16 μm of Pb, appear in Fig. 2. Again, comparison between experiment (curves a, c, and f) and the appropriate Wolfram prediction (curves b′, e, and g) shows reasonable agreement for current steps, good agreement for VSDS structure above eV $\simeq$ 4.0 meV, and poor agreement for VSDS structure below $\simeq$4.0 meV. Now, however, the line shape problem has intensified and unidentified VSDS peaks—the encircled features of curves a and c—have increased from one to four.

Before proceeding, it is helpful to understand why Wolfram's theory remains successful at some biases (energies) but not at others. In his original treatment, Wolfram assumes metal S to be very thick and/or dirty, conditions we refer to as the Wolfram limit. Specifically, quasiparticle currents that enter metal S, reflect from its distant surface, and return to metal N are presumed to scatter incoherently somewhere along this path and are neglected. In this limit, metal S serves only to produce the change in pairing potential ($\simeq\Delta_S-\Delta_N$) needed for Andreev scattering, and neither film thickness, d_S, nor MFP, l_S, appear in $N(E)$. Wolfram's theory should, therefore, successfully describe current steps since, for these, total internal reflection confines quasiparticles to metal N and, thus, renders the scattering properties of metal S irrelevant. At the other extreme, scattering by spontaneous emission of S-metal phonons enforces the Wolfram limit at higher energies, so that even very clean Pb films do not exhibit resonances above eV $\simeq$(4.0 meV + Δ_{CE}).[10,11] Since Wolfram's theory includes strong-coupling effects, his VSDS spectrum should describe Zn-Pb above 4.0 meV. Both expectations are in accord with our observations.

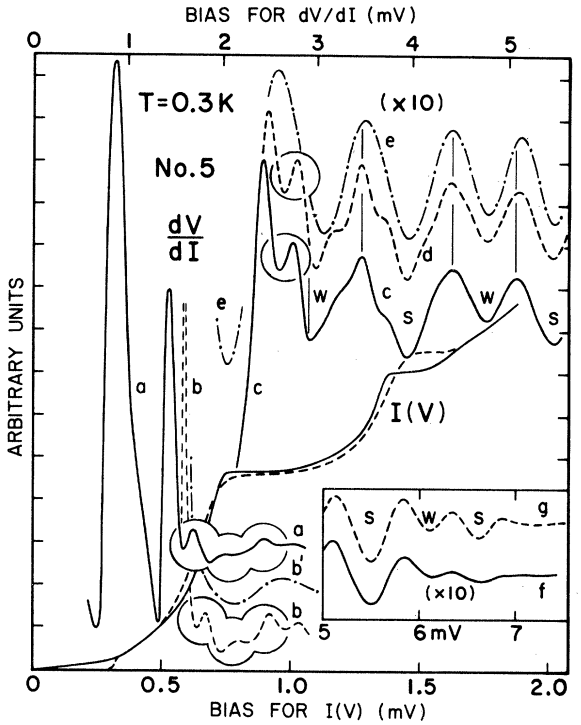

FIG. 2. Tunneling measurements (solid curves) acquired with 1.35 μm of Zn backed by 1.16 μm of Pb. Compound resonances again occur for biases 1.6–4.0 meV. All theoretical results (broken curves) correspond to one value of $C_N Z_N(0)$. Gallagher's prediction (b and d) accounts for low-lying (encircled) virtual states (a and c), and Wolfram's (b′ and e) does not. Both theories produce the same results below $\simeq$1.6 meV and above $\simeq$4.0 meV. Interference between 2d- and 4d-series contributions to $N(E)$ again causes alternations between strong (S) and weak (W) minima, even in the absence of compound resonance effects (f and g).

IV. GALLAGHER THEORY

Gallagher has recently solved Wolfram's model without restricting the amount of S-metal scattering.[6] Although his solution reduces to Wolfram's in the appropriate limit, it otherwise depends on d_S and l_S, and when $\gamma_S=2d_S/l_S\lesssim 1$ holds, it predicts substantial modifications in the VSL spectrum. Interference between geometrical resonances established in each layer now gives rise to a more complicated set of levels characteristic of the composite N-S sandwich as a whole. Gallagher refers to these as compound geometrical resonances.[6]

At the N-metal surface, his density of states[8] for quasiparticles having momenta parallel to the sandwich normal ($k_\parallel=0$) is given by Eq. (1):

$$N(E)=\mathrm{Re}\{D[\epsilon_N\sin\omega_N\cos\omega_S+\epsilon_S\sin\omega_S\cos\omega_N+\delta_N(\epsilon_S\delta_N-\epsilon_N\delta_S)\sin\omega_S(\cos\omega_N-1)]\}\ , \tag{1}$$

where

$$D^{-2}=1-[\cos\omega_N\cos\omega_S-(\epsilon_N\epsilon_S-\delta_N\delta_S)\sin\omega_N\sin\omega_S]^2$$

and the remaining quantities are defined as follows $\omega_M=\pi C_M Z_M(E)\,\Omega_M(E)+i\gamma_M$; $C_M=4d_M/h v_{FM}$; $\Omega_M^2(E)=E^2-\Delta_M^2(E)$; $\epsilon_M=E/\Omega_M(E)$; $\delta_M=\Delta_M(E)/\Omega_M(E)$; and $\gamma_M=2d_M/l_M$. The subscript M denotes either N or S, and v_{FM} denotes the bare band Fermi velocity.

In the Wolfram limit, as $\exp(-\gamma_S)$ vanishes, Eq. (1) reduces to Wolfram's result at all energies. At higher energies ($E >> \Delta_M$) both theories then yield

$$N(E)\simeq \mathrm{Re}[1+\tfrac{1}{2}E^{-2}\Delta_N^2(E)]+E^{-2}\exp(-\gamma_N)\mathrm{Re}\{\Delta_N(E)[\Delta_S(E)-\Delta_N(E)]\exp(iK_NE)\}$$
$$+\tfrac{1}{2}E^{-2}\exp(-2\gamma_N)\,\mathrm{Re}\{[\Delta_S(E)-\Delta_N(E)]^2\exp(2iK_NE)\}\ , \qquad (2)$$

where $K_N=\pi C_N Z_N(E)$. Of these terms the first represents the strong-coupling BCS background; the second and third each represent damped oscillatory series that, together, comprise the VSL spectrum sampled by Giaever tunneling. If one neglects phonon damping in metal N, the first series has an approximate amplitude $|\Delta_N(\Delta_S-\Delta_N)|E^{-2}\exp(-\gamma_N)$ and a quasiperiod $\delta E\simeq h v_{FN}^*(E)(2d_N)^{-1}$, where $v_{FN}^*(E)=v_{FN}/\mathrm{Re}Z_N(E)$ denotes the dressed group velocity. The second series has an approximate amplitude $\frac{1}{2}|\Delta_S-\Delta_N|^2E^{-2}\exp(-2\gamma_N)$ and a quasiperiod $\delta E\simeq h v_{FN}^*(E)(4d_N)^{-1}$. We follow Colucci *et al.*[12] and refer to these as the $2d$ series and $4d$ series. When these harmonically related series are summed, interference causes $N(E)$ to exhibit amplitude alternations (strong, weak, strong, etc.) that carry over to the tunneling spectrum (VSDS) and give rise to the so-called strong-weak effect.[12] Our sandwiches, because of their generally strong structure, are described by small γ_N values and, hence, yield only modest strong-weak effects[12] like those depicted in Figs. 1 and 2.

V. PARAMETER EVALUATION BY CURVE FITTING

Current steps, always confined to low biases, reflect only the low-energy behavior of $N(E)$ and, hence, are treatable within the simplifying approximation $Z_N(E)\approx Z_N(0)$, making them a natural starting point for fitting Gallagher's theory to experiment.[13,14] Although the gap parameter, Δ_N, influences $I(V)$ near $eV=\Delta_{CE}+\Delta_N$, elsewhere, current steps have their heights and bias locations determined, respectively, by γ_N and $C_NZ_N(0)$. Owing to a latitude in possible compromises when fitting $I(V)$, initial estimates of $C_NZ_N(0)$ contain modest uncertainties (5–10%) that can be reduced by fitting computed spectra to our VSDS observations at lower biases ($eV\simeq 1.7$–3.0 meV) where $Z_N(E)=Z_N(0)$ remains useful. In Fig. 1, for example, currents computed for $C_NZ_N(0)$ values of 1.71 and 1.56 $(\mathrm{meV})^{-1}$ (dotted and dashed curves, respectively) both provide acceptable fits to the observed current (solid curve), yet only the latter value permits the good derivative fit depicted by curve d. Final estimates of $C_NZ_N(0)$ retain curve-fitting ambiguities of 1–2%.

The remaining parameters, γ_S and $C_SZ_S(0)$, are inferred from fitting Gallagher's theory to VSDS data taken at biases below 4.0 meV. Reducing γ_S to small values ($\lesssim 1$) tends to emphasize deviations from Wolfram's spectrum, and changing $C_SZ_S(0)$ produces effects resembling those of interference between two series of damped oscillations having quasiperiods $[Z_N(0)C_N]^{-1}$ and $[Z_S(0)C_S]^{-1}$. (These series represent layer resonances and are not to be confused with the $2d$ and $4d$ series that occur even in the Wolfram limit,[12] where the S-layer resonance is absent.) If for simplicity we first assume γ_N to be known, our iterative method for inferring $C_NZ_N(0)$, $C_SZ_S(0)$, and γ_S/γ_N reduces to these steps: (1) An initial estimate of $C_NZ_N(0)$, say from $I(V)$, is used to compute spectra (VSDS) for several plausible choices of $C_SZ_S(0)$ and γ_S/γ_N; (2) best values of these parameters, as inferred from comparisons with observed spectra, are then used to compute new spectra for alternative values of $C_NZ_N(0)$; and (3) the resulting best value of $C_NZ_N(0)$, when returned to step (1), may be used for further parameter refinements. In practice, γ_N can be inferred from any of three experimental considerations: from normalized VSDS amplitudes; from qualitative aspects of the spectrum, such as strong-weak character; and from the strength of step structure in $I(V)$. To achieve agreement with normalized experimental amplitudes, γ_N values may be adjusted during any stage of these computations. Values selected by this criterion provide generally good descriptions of the qualitative features governed by γ_N.

Strong-coupling effects, which determine the complex, energy-dependent character of $\Delta_{N,S}(E)$ and $Z_{N,S}(E)$ at higher energies, must be included when fitting VSDS measurements above $eV\simeq 3.0$ meV. For our Pb layers we assume that $\Delta_S(E)$ and $Z_S(E)$ are adequately approximated by the tunneling results of Rowell, McMillan, and Dynes.[15] Although the bulk Zn gap function is too small to influence $N(E)$, the renormalization computed from the c axis

$\alpha^2F(\omega)$ of Tomlinson and Swihart[7,16] correctly suggests that changes in $Z_N(E)$ are quite significant. We find that both $\mathrm{Re}Z_N(E)$ and $\mathrm{Im}Z_N(E)$ evidence an accelerated increase with increasing energy; and at higher biases, the former produces progressive level crowding[9] and the latter progressive damping. While initial curve-fitting attempts approximate $Z_N(E)/Z_N(0)$ by the computed estimate, subsequent attempts incorporate empirical modifications designed to improve level locations and level amplitudes at higher biases. It is important to bear in mind that, whereas $\lambda_N = Z_N(0) - 1 \simeq 0.42$ may not qualify Zn as a strong-coupling superconductor, our experiment responds sensitively to small absolute changes in $\mathrm{Im}Z_N(E)$, which cause exponentially large damping effects, and to modest relative changes in $\mathrm{Re}Z_N(E)$, which cause substantial phase changes when d_N is sufficiently large.

VI. EXPERIMENT VERSUS GALLAGHER THEORY: A SUMMARY

Comparisons of experimental spectra (Figs. 1 and 2) against their theoretical counterparts (dashed curves b, d, and g) demonstrate the improvements effected by Gallagher's theory; low-lying VSDS peaks, formerly unexplained, are now accounted for; discrepancies in line shapes and level locations (eV $\simeq$ 1.6–4.0 meV) are mainly resolved; choices of γ_N dictated by VSDS amplitudes continue to yield appropriate strong-weak effects; and earlier good agreement above 4.0 meV is retained. Our empirical renormalization, $Z_N(E)/Z_N(0)$, used for all the computations of Figs. 1 and 2, has its real and imaginary parts plotted as solid curves in Fig. 3. These generally exceed the estimates of Tomlinson and Swihart,[7,16] which appear as dashed curves in Fig. 3, and by $E \simeq 6.0$ meV, the difference in $\mathrm{Re}[Z_N(E)/Z_N(0)]$ amounts to about 7%. To indicate the phase effects implied by this difference, curve g of Fig. 1 is decorated with dots (●, ■) that represent bias locations of peaks (●) and dips (■) in the spectrum computed using the Tomlinson-Swihart estimate. Comparison discloses discrepancies of π by eV $\simeq$ 5.5 meV and 2π by eV $\simeq$ 6.5 meV. Although the differences in $\mathrm{Im}[Z_N(E)/Z_N(0)]$ (Fig. 3) appear equally significant, the general smallness of this quantity leads only to minor amplitude discrepancies below eV $\simeq$ 6.0 meV. Otherwise, the Tomlinson-Swihart estimate predicts VSDS structure that persists to eV $\simeq$ 7.0 meV, whereas actual structure ceases by $\simeq$ 6.5 meV. Taken together these results emphasize the direct way in which Giaever tunneling experiments on *N-S* sandwiches probe the electron-phonon interaction at low energies, even for weak-coupling (elemental) superconductors like Zn.

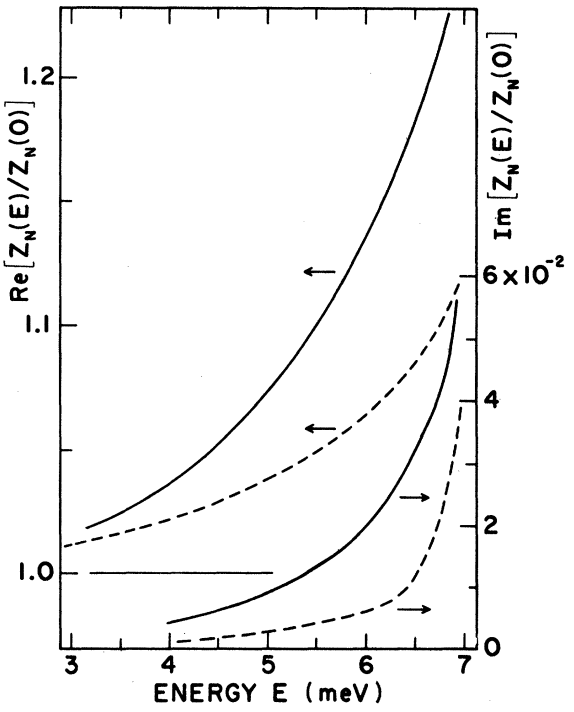

FIG. 3. Real and imaginary parts of the normalized renormalization function, $Z_N(E)/Z_N(0)$, determined empirically (solid curves) from experimental tunneling spectra. Corresponding theoretical quantities (dashed curves) are computed from the c axis $\alpha^2F(\omega)$ given by Tomlinson and Swihart (Ref. 7).

Five of our Zn-Pb sandwiches, labeled as set *B* in Table I, yield agreement comparable to that depicted in Figs. 1 and 2. Although the remaining three sandwiches, set *A*, also produce current steps, none evidence useful VSDS structure above eV $\simeq$ 4.0 meV and, thus, none test $\mathrm{Re}[Z_N(E)/Z_N(0)]$ above $E \simeq 4.0$ meV. Below eV $\simeq$ 4.0 meV, however, both sets of sandwiches produce spectra compatable with our empirical renormalization, $\mathrm{Re}[Z_N(E)/Z_N(0)]$, and both yield quite similar values for $v^*_{FN}(0)$ and for $v^*_{FS}(0)$. Two sandwiches belonging to set *A*, prepared simultaneously, exhibit abrupt declines in amplitude near eV $\simeq$ 4.0 meV; the third produces a steady but rapid decline, so that no structure survives above 3.6 meV. A fourth sandwich, deposited at the same time and on the same substrate as the third, belongs to set *B* and produces VSDS structure that lasts to eV $\simeq$ 6.5 meV. Sandwiches like those of set *A* occur less frequently than their incidence (37%) among our group of eight suggests. Of 23 Zn-Pb evaporations that produced diodes with VSDS structure, only two produced diodes lacking such structure above eV $\simeq$ 4.0 meV. We feel that the evidence warrants viewing this minority damping behavior as

TABLE I. Film thicknesses, MFP values, and Fermi velocities for eight Zn-Pb sandwiches. Fermi velocities, $v_{FM}^{*}(0)=4d_M/hC_MZ_M(0)$, and MFP values, $l_M=2d_M/\gamma_M$, where $M=N$ specifies Zn and $M=S$ specifies Pb, are inferred by fitting Gallagher's theory to our tunneling spectra.

d_N (μm)	d_S (μm)	l_N[a] (μm)	l_N[b] (μm)	l_S (μm)	$v_{FN}^{*}(0)$ (10^6 m/s)	$v_{FS}^{*}(0)$ (10^6 m/s)
2.43[c,d]	0.26	6.9	4.4	2.0	1.30	
2.96[c,e]	1.06	7.4	4.7	2.8	1.32	0.81
2.91[c,e]	0.97	6.9	4.3	2.8	1.30	0.72
1.24[f]	0.25	4.5		5.0	1.26	
1.35[f]	1.16	5.4	2.4	3.3	1.31	0.76
1.52[f]	0.23	4.0	2.9	1.5	1.34	
2.16[f]	1.22	7.2	4.5	3.3	1.33	0.81
2.47[f,d]	0.26	6.9	4.4	0.9	1.31	

[a] Determined from current steps.
[b] Determined from normalized VSDS.
[c] Set *A*: exhibits anomalous damping.
[d,e] Diodes fabricated simultaneously.
[f] Set *B*: exhibits normal damping.

behavior as anomalous. Although abrupt decreases in amplitude near 4.0 meV (observed in two of three instances) could indicate Pb phonon emission and/or Pb pair breaking ($3\Delta_S \simeq 3.9$–4.2 meV), the actual origin of such damping remains moot.

Theoretical currents and corresponding VSDS curves (Figs. 1 and 2) are computed using the same set of parameter values, with one significant exception: current computations employ reduced values of γ_N in order to reproduce the strong step structure observed. In the six instances for which sufficiently complete data exists, these reductions are such that observed VSDS amplitudes, although large, average only two-thirds as large as those anticipated from the current steps. Since current steps result from total internal reflection but VSDS structure results from quasiparticle transmission, such decreases in VSDS amplitudes could indicate that band-structure changes and/or chemical contamination, both localized near the *N-S* interface, cause moderate incoherent scattering.

Film thicknesses and fitting parameters for the eight Zn-Pb sandwiches exhibiting compound resonances are presented in Table I. Within experimental uncertainties, set *A* yields Fermi velocities that coincide with those of set *B*, and the combined sets yield an average Zn velocity of $(1.31 \pm 0.025) \times 10^6$ m/s. This compares favorably with our other determination,[3] $(1.31 \pm 0.015) \times 10^6$ m/s, obtained with a third set of six sandwiches ($d_N = 3.0$–6.2 μm, $d_S = 0.07$–0.27 μm) that exhibit no anomalous damping and only minor compound resonance effects. It also compares favorably with the Tomlinson-Swihart value $(1.29$–$1.32) \times 10^6$ m/s. Based on the extended set of fourteen sandwiches, our best estimate of the *c*-axis Fermi velocity—that is, the velocity at the center of the third-zone lens surface—is $(1.31 \pm 0.020) \times 10^6$ m/s. This value agrees with that obtained by Rahn and Sabo[17] $(1.31 \times 10^6$ m/s) from magnetic surface state measurements on Zn single crystals.

Dividing our measured velocity by the appropriate bare value, that is, by the theoretical rigid-lattice value, v_{FN}, yields a hybrid estimate of $Z_N(0)$. For this purpose we use Tomlinson and Swihart's *c*-axis velocity, 1.86×10^6 m/s, which they compute[7] using a modified form of Stark and Falicov's nonlocal pseudopotential.[18] Our resulting estimate for the superconducting state, $Z_N(0) = 1.42$, falls within the range 1.41–1.44 calculated from first principles by Tomlinson and Swihart.[7,16]

Our Zn results do not, however, agree with those of earlier tunneling studies by Rowell.[1,2] As Colucci *et al.*[12] suggest, the difficulty stems from oversimplifications in Rowell's analysis, which assumes only a $2d$-series contribution to $N(E)$ when metal N is superconducting. Several groups of carriers are then needed to explain observed VSDS complexities that otherwise find a natural, single-carrier explanation within Wolfram's theory.

Owing to experimental uncertainties in the thicknesses of our thinner Pb films, only four of our Zn-Pb sandwiches (those with $d_S = 0.97$–1.22 μm) are used to obtain an average Fermi velocity, $(0.78 \pm 0.04) \times 10^6$ m/s, for the [111] orientation of Pb. This barely overlaps the previous tunneling value, $(0.62 \pm 0.15) \times 10^6$ m/s, determined by Lykken, Geiger, Dy, and Mitchell[11] from VSDS measurements on epitaxial Pb-Ag sandwiches; but agrees more nearly with their theoretical estimate, 0.76×10^6 m/s, based on Anderson and Gold's Fermi surface[19]

and Rowell and McMillan's renormalization.[20]

Taken as a whole, our results emphasize the direct and detailed way in which quasiparticle interference phenomena—as perceived through Giaever tunneling and interpreted by existing model theories—probe the electron-phonon interaction at low energies in clean elemental superconductors, even in weak-coupling superconductors.

ACKNOWLEDGMENTS

We thank J. C. Swihart and Mr. Lee-Tin Cheng for corroborating and, in one instance, for improving our computed renormalizations. We also thank G. B. Arnold for several useful discussions. This work was supported in part by National Science Foundation Grant No. DMR78-12994.

---

*Current address: Texas Instruments, Semiconductor Division, Dallas, Tex. 75222.

[1]J. M. Rowell, Phys. Rev. Lett. 30, 167 (1973).
[2]J. M. Rowell, J. Vac. Sci. Technol. 10, 702 (1973).
[3]S. Shih, L. S. Wong, and W. J. Tomasch (unpublished).
[4]A. F. Andreev, Zh. Eksp. Teor. Fiz. 46, 1823 (1964) [Sov. Phys. JETP 19, 1228 (1964)].
[5]T. Wolfram, Phys. Rev. 170, 481 (1968).
[6]W. J. Gallagher, Phys. Rev. B 22, 1233 (1980).
[7]P. G. Tomlinson and J. C. Swihart, Phys. Rev. B 19, 1867 (1979).
[8]In this and all that follows, $N(E)$ denotes the normalized one-dimensional density of states (per spin) evaluated at the exposed surface of metal N. It does not include proximity-effect modifications.
[9]Z. G. Khim and W. J. Tomasch, Phys. Rev. Lett. 42, 1227 (1979).
[10]W. J. Tomasch, Phys. Rev. Lett. 15, 672 (1965).
[11]G. I. Lykken, A. L. Geiger, K. S. Dy, and E. N. Mitchell, Phys. Rev. B 4, 1523 (1971).
[12]S. L. Colucci, W. J. Tomasch, and Hyung Joon Lee, Phys. Rev. Lett. 32, 590 (1974).
[13]Our procedures for computing $I(V)$ and dV/dI from $N(E)$ are like those used successfully by Khim and Tomasch (Ref. 14) to explain their Al-Pb results in terms of Wolfram's theory. We assume specular tunneling and include the broadening effects of temperature and modulation.
[14]Z. G. Khim and W. J. Tomasch, Phys. Rev. B 18, 4706 (1978).
[15]J. M. Rowell, W. L. McMillan, and R. C. Dynes (unpublished).
[16]J. C. Swihart and Lee-Tin Cheng (private communication).
[17]J. P. Rahn and J. J. Sabo, Jr., Phys. Rev. B 6, 3666 (1972).
[18]R. W. Stark and L. M. Falicov, Phys. Rev. Lett. 19, 795 (1967).
[19]J. R. Anderson and A. V. Gold, Phys. Rev. 139, A 1459 (1965).
[20]W. L. McMillan and J. M. Rowell, in *Superconductivity*, edited by R. D. Parks (Marcel Dekker, New York, 1969), Vol. I, p. 561.